

Mechanisms of nonthermal destruction of the superconducting state and melting of the charge-density-wave state by femtosecond laser pulses

L. Stojchevska,¹ P. Kusar,¹ T. Mertelj,¹ V. V. Kabanov,¹ Y. Toda,^{1,2} X. Yao,³ and D. Mihailovic¹

¹Complex Matter Department, Jozef Stefan Institute, Jamova 39, SLO-1000 Ljubljana, Slovenia

²Department of Physics, Hokkaido University, Sapporo, Japan

³Department of Physics, Shanghai Jiao Tong University, Shanghai 200030, China

(Received 1 September 2011; published 14 November 2011)

The processes leading to nonthermal condensate vaporization and charge-density-wave (CDW) melting with femtosecond laser pulses is systematically investigated in different materials. We find that vaporization is relatively slow ($\tau_v \sim 1$ ps) and inefficient in superconductors, exhibiting a strong systematic dependence of the vaporization energy U_v on T_c . In contrast, melting of CDW order proceeds rapidly ($\tau_m = 50$ –200 fs) and more efficiently. A quantitative model describing the observed systematic behavior in superconductors is proposed based on a phonon-mediated quasiparticle (QP) bottleneck mechanism. In contrast, Fermi-surface disruption by hot QPs is proposed to be responsible for CDW state melting.

DOI: [10.1103/PhysRevB.84.180507](https://doi.org/10.1103/PhysRevB.84.180507)

PACS number(s): 74.25.Gz, 74.25.Dw, 74.25.Jb, 78.47.—p

Photoinduced phase transitions on the subpicosecond time scale in superconductors and other electronically ordered systems have attracted increasing attention in recent years, partly because of the fundamental desire to control collective states of matter with femtosecond laser pulses, partly because of potential applications in ultrafast phase-change memories, and partly because they may reveal some fundamental insight into the mechanism of high-temperature superconductivity. However, to the best of our knowledge, the details of how absorbed photons cause a change of state on ultrafast time scales have so far not been investigated in detail. Recently, a study on $\text{La}_{2-x}\text{Sr}_x\text{CuO}_4$ (LSCO) single crystals by Kusar *et al.*¹ showed that the energy required to vaporize the superconducting (SC) condensate U_v can be determined with reasonable accuracy. These and other measurements on cuprate superconductors since then^{2–4} give values of U_v which are sometimes significantly larger than the experimental condensation energy U_c , or the BCS theoretical values,⁵ opening the question as to what is the mechanism for the destruction of the condensate, the dependence of U_v on doping, and on the critical temperature T_c . It is also not clear if this occasional large discrepancy between U_c and U_v is a peculiar feature of cuprate superconductors, if it is a consequence of a large gap in the density of states, or of it depends on the detailed mechanism responsible for the formation of the low-temperature ordered state.

To try and answer these questions, we present a first systematic study of the dependence of U_v on doping and T_c for cuprates and compare our data with the iron pnictides [$\text{Ba}(\text{Fe}_{0.93}\text{Co}_{0.07})_2\text{As}_2$ and $\text{SmFeAsO}_{0.8}\text{F}_{0.2}$], the conventional superconductor NbN, and two large-gapped charge-density-wave (CDW) systems $\text{K}_{0.3}\text{MoO}_3$ and TbTe_3 . We made a special effort to determine the geometrical factors and optical constants as accurately as possible in order to achieve the best possible accuracy in determining U_v . We find that the observed systematic behavior reveals the mechanism for breaking up the collective state in high- T_c superconductors to be relatively inefficient and phonon dominated. This is in stark contrast to CDW systems, where the electronic destruction mechanism

is faster, more direct, and efficient. We present a model to describe the observed systematics in the cuprates and discuss the markedly different mechanisms for the photonic destruction of the low-temperature ordered state in the two types of systems.

Our experiments were performed using a standard pump-probe technique with a 800-nm laser with 50-fs pulses as described in Ref. 1. A probe wavelength of 800 nm is chosen because it is a well-understood probe wavelength for investigating the superconducting (SC) and pseudogap (PG) response in pump-probe experiments and has the best signal-to-noise ratio as determined by previous studies. The two-component response, PG and SC, including lifetimes, T dependence, anisotropy, and doping dependence, have been previously studied at 800 nm and other pump-probe wavelengths as well, including pump and probing in the THz region. The results of these measurements are quantitatively self-consistent, and have all been systematically discussed. The second reason for using 800 nm (1.5 eV) is that the optical constants are better known more accurately at this wavelength than any other, which improves the accuracy of the determination of the vaporization energy. The reason for not using far infrared (FIR) wavelengths in the gap region is that even with transform-limited pulses, the pulses become too long to be able to distinctly detect the SC component and distinguish it from the PG. Hence THz or FIR pulses in the gap region are not suitable for our purpose. Recently the electron distribution function thermalization has been measured to be ~ 60 fs in LSCO and ~ 100 fs in $\text{YBa}_2\text{Cu}_3\text{O}_{7-\delta}$ (YBCO),⁶ while the quasiparticle (QP) signal used for detection of the presence of the superconducting state in the cuprates has a characteristic lifetime nearly two orders of magnitude longer and can thus be easily distinguished from the PG and energy relaxation, which are both much faster. In order to accurately determine the deposited energy, pump and probe laser beam diameters were accurately measured with calibrated pinholes. The light penetration depth λ_{op} and reflectivity R are obtained from published optical conductivity and dielectric function data in each case.⁷ The measurements were performed on

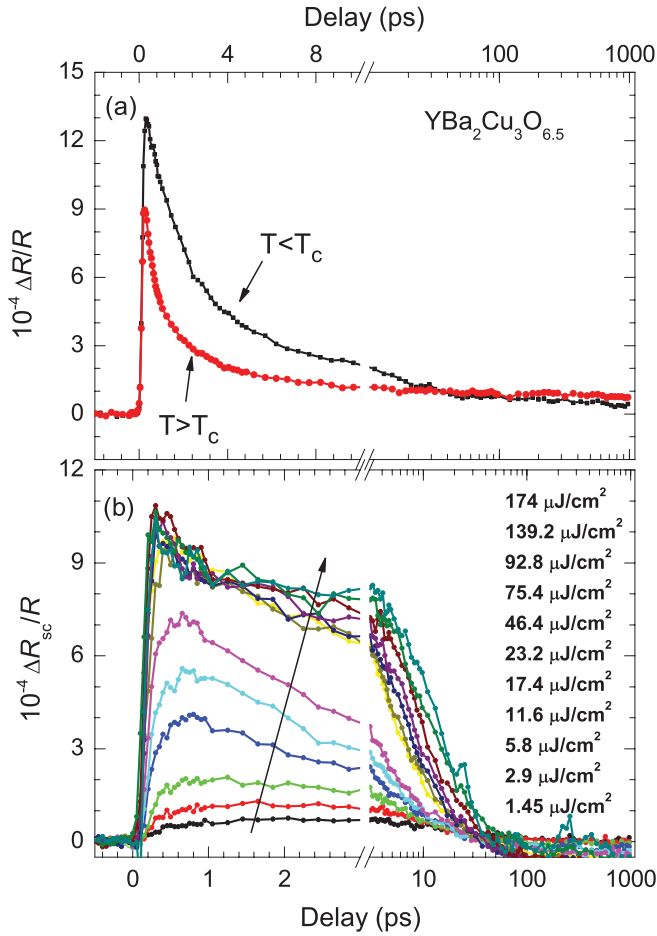


FIG. 1. (Color online) (a) $\Delta R/R$ for $\text{YBa}_2\text{Cu}_3\text{O}_{6.5}$ for $T < T_c$ (squares) and for $T > T_c$ (circles) at excitation fluence $\mathcal{F} = 17.4 \mu\text{J}/\text{cm}^2$. (b) $\Delta R_{sc}/R$ for $\text{YBa}_2\text{Cu}_3\text{O}_{6.5}$ as a function of time delay for different \mathcal{F} , showing saturation above $46 \mu\text{J}/\text{cm}^2$. The arrow indicates the direction of increasing \mathcal{F} . The condensate vaporization time τ_v is between 0.5 and 1 ps. (At high fluences the PG signal interferes with the measurement, so τ_v cannot be more accurately measured in YBaCuO .)

freshly cleaved $\text{YBa}_2\text{Cu}_3\text{O}_{7-\delta}$ single crystals with T_c 's of 90, 63, and 60 K, respectively, and $\text{Ca}_x\text{Y}_{1-x}\text{Ba}_2\text{Cu}_3\text{O}_{7-\delta}$ with $x = 0.132$, $\delta = 0.072$, and $T_c = 73$ K. The photoinduced reflectivity transient $\Delta R/R$ for $\text{YBa}_2\text{Cu}_3\text{O}_{6.5}$ well below T_c (4 K) and above T_c (at 68 K) are shown in Fig. 1(a) while the net superconducting signal, obtained by subtracting the response at $T = 68$ K from the response at $T = 4$ K, $\Delta R_{sc}/R = \Delta R/R|_{T < T_c} - \Delta R/R|_{T > T_c}$, is plotted in Fig. 1(b) for different laser pump pulse fluences. This behavior is generic, so we have shown the raw data only for one sample. $\Delta R_{sc}/R$ shows a saturation plateau above $\mathcal{F} \gtrsim 100 \mu\text{J}/\text{cm}^2$,¹ which is a signature of the destruction of the SC state.

The normalized magnitude of $\Delta R_{sc}/R$ for different materials and different doping levels as a function of \mathcal{F} is shown in Fig. 2. At low fluence $\Delta R_{sc}/R$ is linearly dependent on \mathcal{F} up to a certain threshold fluence \mathcal{F}_T , whereupon it either becomes saturated or continues increasing, but with a different slope. To determine the vaporization threshold fluence \mathcal{F}_T from the data in Fig. 2, we use the inhomogeneous excitation model.⁸ To take

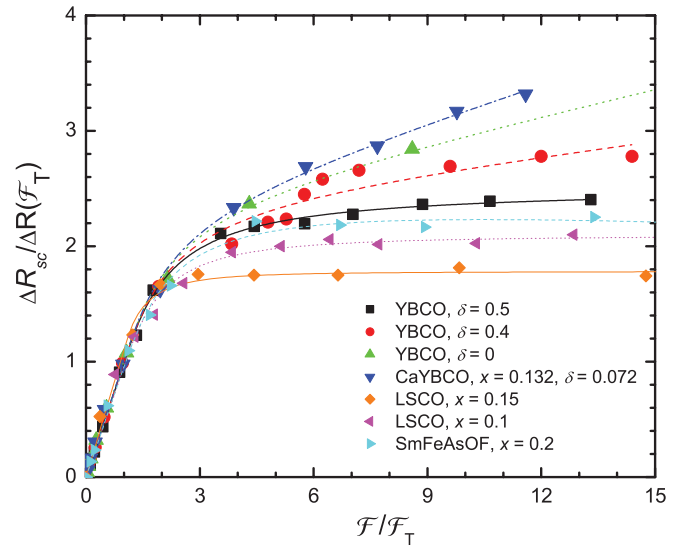


FIG. 2. (Color online) ΔR_{sc} as a function of normalized fluence $\mathcal{F}/\mathcal{F}_T$. Note the linear response below \mathcal{F}_T .

into account the carrier-density-dependent change of $\Delta R/R$ arising from e - h asymmetry in the band structure, we have also included a linear term in the fit to the data in Fig. 2, such that $\Delta R/\Delta R_s = \Delta R_{sc}/\Delta R_s + \phi(\mathcal{F})$. Empirically, we find that in LSCO, $\phi \simeq 0$,¹ while in YBCO samples $\phi(\mathcal{F}) \simeq \phi_0 \mathcal{F}$, where ϕ_0 is a constant. Note that this term has *no effect* on the values of \mathcal{F}_T obtained from the fits to the data in Fig. 2. (As a check, \mathcal{F}_T can also be directly read out as the point where $\frac{\Delta R_{sc}(\mathcal{F})}{R}$ departs from linearity.)

A plot of the vaporization energy $U_v = (1 - R)\mathcal{F}_T/\lambda_{op}$ obtained for cuprates, the iron pnictides, and NbN is shown in Fig. 3. We observe a systematic increase of U_v with T_c , giving an approximate square power-law dependence $U_v = \eta T_c^2$, with $\eta \simeq 1.5 \times 10^{-3} \text{ K}^{-2} \text{ atom}^{-1}$, irrespective of whether the material is overdoped, optimally doped, or underdoped.

In Table I compare U_v with the condensation energy U_c^{exp} obtained from specific-heat measurements. In the cuprates, we notice a significant discrepancy between the magnitudes of U_v and U_c^{exp} . While U_c^{exp} shows a distinct asymmetry between overdoped and underdoped materials with the same T_c ,⁹ U_v depends systematically on T_c , irrespective of doping level. Thus U_v and U_c^{exp} show fundamentally different systematics.

To understand this apparent discrepancy between the condensation and vaporization energy, let us now consider the mechanism of energy transfer between photoexcited (PE) carriers and the condensate. After absorption of a photon, the PE electrons and holes lose energy very rapidly through “avalanche” scattering with phonons on a time scale of $\tau_E < 100$ fs for YBCO and < 60 fs for LSCO,¹⁹ creating a large nonequilibrium phonon population in the process. The phonons whose energy exceeds the gap $\hbar\omega_{\text{ph}} > 2\Delta$ can subsequently excite QPs from the condensate, but these recombine again and so a bottleneck occurs in which high-frequency phonons are temporarily in quasiequilibrium with QPs, as described by Kusar *et al.* for LaSrCuO .¹ The process eventually causes the destruction of the condensate within 0.5–1 ps.¹

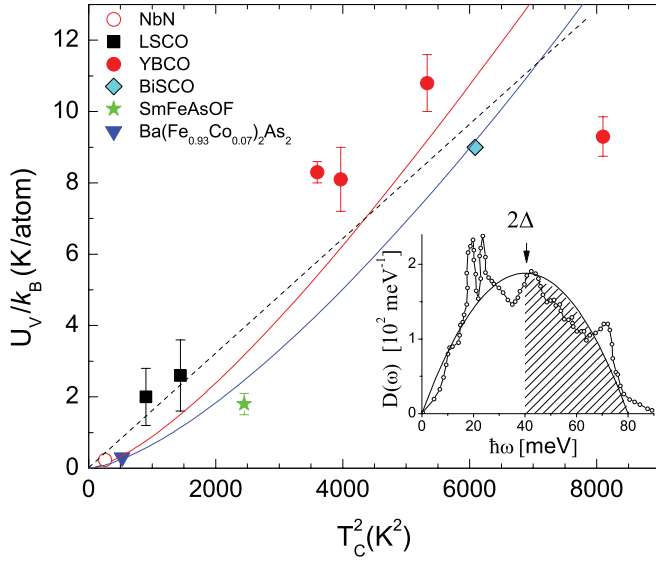


FIG. 3. (Color online) ΔU_v expressed in K per planar Cu as a function of T_c^2 for the cuprates. The data for NbN, SmFeAsO_{0.8}F_{0.2}, and Ba(Fe_{0.93}Co_{0.07})₂As₂ are included for comparison (in K/Fe or K/Nb). The solid curve is a plot of U_{lost} using $D(\omega_{\text{ph}})$ appropriate from Eq. (2) for YBaCuO (red/gray) and the iron oxy-pnictide (blue/dark gray). The dashed line is a square law $U_v = \eta T_c^2$. The inset shows the phonons with $\hbar\omega > 2\Delta$ (shaded) which can break pairs. The measured phonon density of states $D(\omega_{\text{ph}})$ for YBCO (Ref. 20) is approximated by a parabola (line).

The phonons with $\hbar\omega > 2\Delta$ can contribute to the breakup of the condensate, but the *low-frequency* phonons with $\hbar\omega < 2\Delta$ also created in the initial avalanche do not have enough energy

to excite QPs, so they do not contribute to the vaporization process. This lost energy to low-energy phonons is

$$U_{\text{lost}} = \int_0^{2\Delta} \Delta f(\omega) D(\omega) \hbar\omega d\omega, \quad (1)$$

where $D(\omega)$ is the phonon density of states and $\Delta f(\omega) = f_{NE}(\omega) - f_E(\omega)$ is the difference between the nonequilibrium and equilibrium phonon distribution functions. $\Delta f(\omega)$ is material dependent and depends on the electron phonon coupling, more precisely, on the Eliashberg coupling function $\alpha^2 F(\omega)$, but it is not a very strong function of ω .¹⁹ To estimate the dependence of U_{lost} on T_c from Eq. (1), we assume that $\Delta f(\omega)$ is constant, and we approximate the experimental $D(\omega)$ by an inverted parabola $D(\omega) = \frac{\alpha}{8} \omega(2\omega_0 - \omega)$, where α is a constant. Integrating Eq. (1), we obtain

$$U_{\text{lost}} = \alpha \Delta^3 \left[\frac{2\hbar\omega_0}{3} - \frac{\Delta}{2} \right]. \quad (2)$$

Assuming a constant gap ratio $2\Delta/k_B T_c = R$, with $R = 4$, for YBCO, $\hbar\omega_0 = 40$ meV,²⁰ extending $D(\omega)$ to 80 meV as shown in the inset to Fig. 3. Equation (2) gives the curve shown in Fig. 3. For iron pnictides, $\hbar\omega_0 \simeq 20$,²¹ but the predicted variation of U_{lost} on T_c is not significantly different. We see that for the superconductor series Eq. (2) predicts the dependence of U_v on T_c very well, which is not surprising, considering the gross features of $D(\omega)$ do not vary significantly.

The total vaporization energy is the sum of the condensation energy and the lost energy $U_v = U_c + U_{\text{lost}}$. Since for large-gap systems $U_v \gg U_c^{\text{exp}}$ we have $U_v \simeq U_{\text{lost}}$, so U_c^{exp} is thus only a small contribution to U_v , explaining why the anomalous

TABLE I. T_c , \mathcal{F}_T , U_v , and U_c for different materials. U_c and U_v are calculated per metal atom of Cu (planar), Fe, Nb, Tb, or Mo. For LSCO and YBCO, the data for U_c are maximum experimentally measured values (Ref. 9). δ in YBCO was changed by annealing in flowing oxygen, while T_c 's were determined from magnetization measurements. For TbTe₃ and K_{0.3}MoO₃, the electronic part of U_e of the condensation energy is estimated using available values of Δ and N_0 (Refs. 10,12). For YBa₂Cu₃O_{7- δ} , the penetration depths are (Ref. 7) 66 ± 15 nm ($\delta = 0$), 85 ± 15 nm ($\delta = 0.4$), 90 ± 15 nm ($\delta = 0.5$), and 75 ± 15 nm for CaYBCO.

Material	T_c (K)	\mathcal{F}_T ($\mu\text{J}/\text{cm}^2$)	λ_{op} (nm)	U_v	U_c^{exp}	U_v/U_c^{exp}	τ_v (ps)	
La _{1.85} Sr _{0.15} CuO ₄ (opt) (Ref. 1)	38.5	5.8 ± 2.3	150	2.6 ± 1.0 K/Cu	0.3 K/Cu (Ref. 1)	> 8.5	0.9	
YBa ₂ Cu ₃ O _{6.5} (ud)	60	13.1 ± 0.5	90	8.3 ± 0.3 K/Cu	0.38 K/Cu (Ref. 9)	22	0.5–1	
YBa ₂ Cu ₃ O _{6.6} (ud)	63	12.1 ± 1.3	85	8.1 ± 0.9 K/Cu	0.45 K/Cu (Ref. 9)	18		
YBa ₂ Cu ₃ O ₇ (opt)	90	10.8 ± 0.6	66	9.3 ± 0.5 K/Cu	1.9 K/Cu (Ref. 9)	5		
Y _{0.8} Ca _{0.2} Ba ₂ Cu ₃ O _{6.9} (od)	73	14.3 ± 1	75	10.8 ± 0.8 K/Cu	1.4 K/Cu (Ref. 9)	7.7		
Bi ₂ Sr ₂ CaCu ₂ O _{8+δ} (ud) (Ref. 3)	78	16 ± 1	124	9 ± 0.8 K/Cu	1.8	5		
SmFeAsO _{0.8} F _{0.2} (Refs. 13 and 14)	49.5	2.6 ± 0.2	31	1.8 ± 0.1 K/Fe	–	–	0.3–0.5	
Ba(Fe _{0.93} Co _{0.07}) ₂ As ₂	23	0.43 ± 0.04	34	0.3 ± 0.03 K/Fe	0.15 ± 0.02 (Ref. 15)	2	0.5	
NbN (Ref. 4)	16	$U_v = 23 \text{ mJ}/\text{cm}^3$		0.24 K/Nb	0.14 K/Nb	1.7		
	T_c (K)	\mathcal{F}_T ($\mu\text{J}/\text{cm}^2$)		U_m	U_c^{exp}	U_e^{theory}	U_v/U_e	τ_m
TbTe ₃ (Refs. 10 and 16)	336	47 ± 2		52 ± 2 K/Tb	–	40.6 ± 1.7 K/Tb	1.3	0.2 (Ref. 10)
K _{0.3} MoO ₃ (Refs. 12,17 and 18)	180	105 ± 17.5		35 ± 10 K/Mo	>10 K/Mo	30 ± 10 K/Mo (Ref. 17)	1.1 ~ 3.5 (Ref. 17)	0.05–0.1 (Ref. 17)

doping dependence of U_c^{exp} in the cuprates is not displayed by U_v .

Comparing U_v for NbN measured using the same technique (Table I), $U_v/U_c^{\text{exp}} = 1.7$ is considerably smaller than in the cuprates, which can now be understood in terms of Eq. (1) and the inset to Fig. 3: When $2\Delta \ll \hbar\omega_{\text{Debye}}$ almost all phonons can excite QPs, so $U_{\text{lost}} \rightarrow 0$ and $U_v \simeq U_c$, in agreement with the data. For small-gap superconductors, the optical method can be used to estimate the superconducting condensation energy. The data on the two iron pnictides listed in Table I also seem to follow the predicted behavior in Fig. 3.

We now turn our attention to the data obtained using the same technique on two different charge-density-wave materials TbTe₃ and K_{0.3}MoO₃. Both have CDW gaps which are much larger than any phonon energy: $2\Delta_{\text{CDW}} \gg \hbar\omega_D$ ($\Delta_{\text{CDW}} = 125$ and 75 meV, respectively^{11,18}). K_{0.3}MoO₃ is considered to be a prototypical Peierls system with a full gap in the electronic density of states opening at the metal-insulator transition¹⁸ Moreover, in KMo_{0.3}O₃ the electron-phonon coupling constant ($\lambda_{e-p} \simeq 0.35$) is comparable with the cuprates ($\lambda_{e-p} \simeq 0.25$ for YBaCuO and $\lambda_{e-p} = 0.5$ for LSCO, respectively),^{6,18} so with a phonon-mediated CDW melting mechanism we would expect a very large U_m/U_c ratio. Instead, it is significantly *smaller* than in the large-gapped cuprates, with $U_m/U_c^{\text{exp}} \simeq 3.5$. In TbTe₃ the ordered state opens a partial gap only along certain directions on the Fermi surface, with the rest remaining ungapped.¹⁰ Thus, if the same phonon-mediated vaporization mechanism were operative, the ungapped CDW system should behave very differently to KMo_{0.3}O₃ on the one hand and the superconductors on the other. Comparing U_v with the electronic contribution to the CDW condensation energy,^{17,18} $U_e = N_0\Delta^2(\frac{1}{2} + \log \frac{2E_F}{\Delta})$, where E_F is the Fermi energy,¹⁰ we see in Table I that the predicted ratios are $U_m/U_e \simeq 1.3$ for TbTe₃ and 1.1 for K_{0.3}MoO₃, confirming that $U_{\text{lost}} \rightarrow 0$ and implying that phonons are not significantly involved in the CDW gap destruction and CDW melting process. Thus, in spite of a similar $e-p$ interaction strength and very large gaps, U_m/U_c is consistently smaller in the CDWs than U_v/U_c in cuprates, highlighting the very different mechanism for the destruction of the low-temperature CDW state.

The reason is fundamental: Unlike in superconductors, PE carriers in CDW systems can cause a direct rapid disturbance of the Fermi surface¹⁶ on a time scale that is shorter than the QP recombination time. It is known experimentally²² and theoretically²³ that the CDW state is extremely sensitive to charge imbalance, which disrupts the Fermi surface (FS) nesting. In photoexcitation experiments, overall charge neutrality is preserved, but immediately after photon absorption, even the slightest electron-hole band asymmetry causes a transient shift of the chemical potential, causing a disturbance δq of the FS. This causes a destruction of the nesting at k_F and a suppression of the divergence of the electronic susceptibility at $2k_F$ causing the electronic charge density wave to rapidly melt.^{23,24} A fast destruction time in CDWs is experimentally confirmed: In K_{0.3}MoO₃, $\tau_m = 50\text{--}100$ fs,¹⁷ which is an order of magnitude less than $\tau_v \sim 0.9$ ps in LaSCO, which has a similar $e-p$ interaction strength. Indeed, quite generally, the melting time τ_m is significantly shorter than the τ_v in superconductors, as shown in Table I (not all rise times are reliably measured so far, so only the unambiguous ones are listed). With $\tau_m = 50\text{--}100$ fs, the ions can just barely move into different equilibrium positions within this time, (the 1/4 period of the amplitude mode in K_{0.3}MoO₃ is ~ 150 fs).^{11,25,26}

We conclude that a photon-induced change of state in superconductors and CDW systems relies on very different mechanisms, occurring on different time scales and requiring different amounts of energy. Systematic and experimentally precise measurements of the dependence of U_v on doping and on T_c in cuprates, pnictides, and low- T_c superconductors show that vaporization can be described by the established Rothwarf-Taylor QP recombination mechanism, in a process whereby energy transfer to the condensate is slowed down and made inefficient by the phonon-QP relaxation bottleneck. In CDW systems, on the other hand, the dominant mechanism for the destruction of the ordered state is electronic, so in spite of the fact that the CDW gaps $2\Delta_{\text{CDW}}$ are typically much larger than the highest phonon frequencies, and electron-phonon coupling strengths are similar as in cuprates, the destruction is faster and more direct.

¹P. Kusar, V. V. Kabanov, S. Sugai, J. Demsar, T. Mertelj, and D. Mihailovic, *Phys. Rev. Lett.* **101**, 227001 (2008).

²G. Coslovich *et al.*, e-print [arXiv:1005.4320v1](https://arxiv.org/abs/1005.4320v1).

³Y. Toda *et al.* (unpublished).

⁴C. Geibel, H. Rietschel, A. Junod, M. Pelizzone, and J. Muller, *J. Phys. F* **15**, 405 (1985). \mathcal{F}_T is given by M. Beck *et al.* (unpublished).

⁵J. Bardeen, L. N. Cooper, and J. R. Schrieffer, *Phys. Rev.* **108**, 1175 (1957).

⁶C. Gadermaier, A. S. Alexandrov, V. V. Kabanov, P. Kusar, T. Mertelj, X. Yao, C. Manzoni, D. Brida, G. Cerullo, and D. Mihailovic, *Phys. Rev. Lett.* **105**, 257001 (2010).

⁷S. L. Cooper, D. Reznik, A. Kotz, M. A. Karlow, R. Liu, M. V. Klein, W. C. Lee, J. Giapintzakis, D. M. Ginsberg, B. W. Veal, and A. P. Paulikas, *Phys. Rev. B* **47**, 8233 (1993).

⁸See the Supplemental Material for Ref. 1, available via E-PRLTAO-101-090848 at [<http://www.aip.org/pubservs/epaps.html>].

⁹J. W. Loram, J. Luo, J. R. Cooper, W. Y. Liang, and J. L. Tallon, *J. Phys. Chem. Solids* **62**, 59 (2001); R. Lortz, A. Junod, D. Jaccard, Y. Wang, C. Meingast, T. Masui, and S. Tajima, *J. Phys. Condens. Matter* **17**, 4135 (2005).

¹⁰The value of $N(E)$ for TbTe₃ is from J. Laverock, S. B. Dugdale, Z. Major, M. A. Alam, N. Ru, I. R. Fisher, G. Santi, and E. Bruno, *Phys. Rev. B* **71**, 085114 (2005), and Δ from Ref. 11.

¹¹R. V. Yusupov, T. Mertelj, J. H. Chu, I. R. Fisher, and D. Mihailovic, *Phys. Rev. Lett.* **101**, 246402 (2008).

¹²R. S. Kwok and S. E. Brown, *Phys. Rev. Lett.* **63**, 895 (1989).

¹³T. Mertelj, V. V. Kabanov, C. Gadermaier, N. D. Zhigadlo, S. Katrych, J. Karpinski, and D. Mihailovic, *Phys. Rev. Lett.* **102**, 117002 (2009).

- ¹⁴T. Mertelj, P. Kusar, V. V. Kabanov, L. Stojchevska, N. D. Zhigadlo, S. Katrych, Z. Bukowski, J. Karpinski, S. Weyeneth, and D. Mihailovic, *Phys. Rev. B* **81**, 224504 (2010).
- ¹⁵G. P. Segre, N. Gedik, J. Orenstein, D. A. Bonn, R. Liang, and W. N. Hardy, *Phys. Rev. Lett.* **88**, 137001 (2002).
- ¹⁶R. Yusupov, T. Mertelj, V. V. Kabanov, S. Brazovskii, P. Kusar, J. H. Chu, I. R. Fisher, and D. Mihailovic, *Nat. Phys.* **6**, 681 (2010).
- ¹⁷A. Tomeljak, H. Schafer, D. Stadter, M. Beyer, K. Biljakovic, and J. Demsar, *Phys. Rev. Lett.* **102**, 066404 (2009).
- ¹⁸G. Gruner, *Rev. Mod. Phys.* **60**, 1129 (1988).
- ¹⁹V. V. Kabanov and A. S. Alexandrov, *Phys. Rev. B* **78**, 174514 (2008); P. B. Allen and B. Mitrovic, *Solid State Phys.* **37**, 1 (1982).
- ²⁰B. Renker *et al.*, *Physica B* **165-166**, 1237 (1990).
- ²¹M. Le Tacon, M. Krisch, A. Bosak, J. W. G. Bos, and S. Margadonna, *Phys. Rev. B* **78**, 140505(R) (2008).
- ²²S. Girault, A. H. Moudden, J. P. Pouget, and J. M. Godard, *Phys. Rev. B* **38**, 7980 (1988).
- ²³X. Huang and K. Maki, *Phys. Rev. B* **42**, 6498 (1990).
- ²⁴F. Schmitt, P. S. Kirchmann, U. Bovensiepen, R. G. Moore, L. Rettig, M. Krenz, J. H. Chu, N. Ru, L. Perfetti, D. H. Lu, M. Wolf, I. R. Fisher, and Z. X. Shen, *Science* **321**, 1649 (2008).
- ²⁵M. Eichberger, H. Schafer, M. Krumova, M. Beyer, J. Demsar, H. Berger, G. Moriena, G. Sciaimi, and R. J. Dwayne Miller, *Nature (London)* **468**, 799 (2010).
- ²⁶C. Giannetti, G. Coslovich, F. Cilento, G. Ferrini, H. Eisaki, N. Kaneko, M. Greven, and F. Parmigiani, *Phys. Rev. B* **79**, 224502 (2009).